ELSEVIER

Biophysical Chemistry 134 (2008) 25–33

Biophysical Chemistry

http://www.elsevier.com/locate/biophyschem

Myoglobin immobilization on electrodeposited nanometer-scale nickel oxide particles and direct voltammetry

Abdolmajid Bayandori Moghaddam [a], Mohammad Reza Ganjali [a,*], Rassoul Dinarvand [b], Sara Ahadi [a], Ali Akbar Saboury [c]

[a] *Center of Excellence in Electrochemistry, Faculty of Chemistry, University of Tehran, P. O. Box 14155-6455, Tehran, Iran*
[b] *Medical Nanotechnology Research Centre, Medical Sciences/University of Tehran, Tehran, P.O. Box 14155-6451, Iran*
[c] *Institute of Biochemistry and Biophysics, University of Tehran, Tehran, Iran*

Received 27 November 2007; received in revised form 6 January 2008; accepted 7 January 2008
Available online 12 January 2008

Abstract

Prosperity of information on the reactions of redox-active sites in proteins can be attained by voltammetric studies in which the protein sample is located on a suitable surface. This work reports the presentation of myoglobin/nickel oxide nanoparticles/glassy carbon (Mb/NiO NPs/GC) electrode, ready by electrochemical deposition of the NiO NPs on glassy carbon electrode and myoglobin immobilization on their surfaces by the potential cycling method. Images of electrodeposited NiO NPs on the surface of glassy carbon electrode were obtained by scanning electron microscopy (SEM) and atomic force microscopy (AFM). A pair of well-defined redox peaks for Mb(Fe(III)–Fe(II)) was obtained at the prepared electrode by direct electron transfer between the protein and nanoparticles. Electrochemical parameters of immobilized myoglobin such as formal potential ($E^{0'}$), charge transfer coefficient (α) and apparent heterogeneous electron transfer rate constant (k_s) were estimated by cyclic voltammetry and nonlinear regression analysis. Biocatalytic activity was exemplified at the prepared electrode for reduction of hydrogen peroxide.

Keywords: Myoglobin; Nanotechnology; Atomic force microscopy; Bioelectrochemistry; Nanoparticle; Nickel oxide

1. Introduction

The rapid advances in nanoscience introduced a scientific elevation that involves the fundamental understanding of the properties of nanostructures, synthesis and imaging of nanometer-scale materials and assembly of nanometer-scale devices [1,2]. They have provided a variety of nanostructured materials with unique optical [3], electrical [4], magnetic [5] and catalytic properties [6]. The diversity in composition, shape and the readiness for surface functionalization has enabled the fabrication of various functional nanometer-scale materials for biointerfaces [7,8].

Regarding the fundamental investigations of the biological redox reaction mechanism and the development of biodiagnostics and bioelectronic devices, the achievement of an interface between the prosthetic groups of immobilized proteins/enzymes of redox proteins and an electrode surface is presently a research frontier [9–14]. The redox reaction kinetics of proteins on an electrode is known to be strongly dependent upon a combination of interfacial electrostatic and chemical interactions, which are derived from protein structure and the nature of electrode surface.

Myoglobin (Mb) is a single-chain protein of 153 amino acids containing a heme (iron-containing porphyrin) group in the center. Mb is found in mammalian skeleton and muscle tissues which functions in the storage of oxygen and in the enhancement of the rate of oxygen diffusion [15,16]. Because the heme group in Mb is much more buried with respect to the protein surface than in cytochrome its interaction with the electrode surface is hindered [17].

Initially, redox proteins (e.g. cytochrome *c*) were believed to be incapable of exhibiting a voltammetric response because of the extremely slow electron-transfer kinetics at the electrode/

* Corresponding author. Tel.: +98 21 61112788; fax: +98 21 66405141.
E-mail address: ganjali@khayam.ut.ac.ir (M.R. Ganjali).

0301-4622/$ - see front matter © 2008 Elsevier B.V. All rights reserved.
doi:10.1016/j.bpc.2008.01.001

solution interface. However, in 1977, Yeh and Kuwana reported a direct and rapid electron transfer between cytochrome *c* and a tin-doped indium oxide electrode surface [18]. In the same year, Hill and Eddowes demonstrated that the voltammetry of cytochrome *c* was well defined at a gold electrode modified with 4,4′-bipyridil [19].

Since that time, electrochemical devices have opened up new possibilities for studying the redox process of cytochrome *c* and related heme proteins [20–22]. Many reports have described the electrochemistry of Mb using electrodes modified with films such as inorganic materials [23–30], surfactants [31–33], polymers [34,35], multi-walled carbon nanotube [36,37], gold nanoparticles [38,39], with a boron-doped diamond electrode [40] and zirconia deposited electrode [41] has been reported. Furthermore, direct electron transfer of Mb in methanol and ethanol at didodecyldimethylammonium bromide modified pyrolytic graphite electrode has been reported [42].

As far as nano-materials are concerned, they offer attractive properties and they open a new entrance for new electrodes in the field of electrochemical applications [43]. Metal nanoparticles (NPs) are employed as versatile labels for the optical or electrical detection of biorecognition events or biocatalytic transformations [44].

A literature survey shows that several studies have been devoted to the investigation of the nickel electrode electrochemistry for a number of applications: as a model for studying the oxygen-evolution reaction [45,46], the oxidation of organic compounds at passivated nickel anodes [47], electroanalytical approach based on the interaction of sulphide with an electrochemically generated nickel oxide layer [48–54] as well as the production of different phases of nickel sulphide nanocrystals from the reaction of nickel metal nanoparticles supported on graphitized carbon with hydrogen sulphide [55]. Moreover, an anodic stripping voltammetric method for sub-speciation of Ni_3S_2, NiS and NiS_2 in the mixtures of carbon paste electrodes in an acetate buffer [56], the electrochemically deposited nickel microparticles onto a carbon substrate for sulphide detection [57], modification of glassy carbon electrode by the nickel oxide nanoparticles for the immobilization of hemoglobin, catalase, glucose oxidase and cytochrome *c* [11,58–60] and use of Ni/NiO for the preparation of silicon nanotube array/gold electrode for the direct electrochemistry of cytochrome *c* [61].

In total, this paper introduces an electrochemical investigation on redox reaction of the immobilized myoglobin as myoglobin/nickel oxide nanoparticles/glassy carbon electrode (Mb/NiO NPs/GC electrode).

2. Experimental details

2.1. Chemicals and reagents

Myoglobin (Mb, from equine skeletal muscle) was purchased from Sigma. The phosphate buffer solution (PBS) consisted of a potassium phosphate solution (KH_2PO_4 and K_2HPO_4 from Merck; 0.05 M total phosphate) at pH 7.0. An acetate buffer solution (CH_3COONa and CH_3COOH from Merck; 0.05 M) was freshly prepared. $Ni(NO_3)_2.6H_2O$ and the other reagents were reagent grade materials from Merck. Deionized water was used to prepare all solutions and to rinse the electrodes.

2.2. Apparatus and procedure

Electrochemical measurements were executed by the Autolab potentiostat PGSTAT 30 (Eco Chemie B.V., Netherlands), equipped with the GPES 4.9 software. A three-electrode single-compartment voltammetric cell [62–65] was also used, employing a glassy carbon (GC) electrode or modified-GC electrodes, acting as the working electrode. A platinum wire was applied as the counter electrode and Ag/AgCl was applied as the reference electrode (KCl-saturated, 0.197 V versus a normal hydrogen electrode, NHE). All potentials were reported with respect to this reference. All experiments were performed at 25 ± 1 °C.

Prior to the myoglobin immobilization, the glassy carbon electrode (2 mm in diameter) surface along with the alumina slurry surfaces of 1.0, 0.3 and 0.05 μm were polished, former to a mirror-like one with fine emery papers and the latter with a polishing cloth, followed by a thorough deionized water rinsing. The electrode was then successively sonicated in ethanol and doubly distilled water to remove the adsorbed particles. Then, cyclic scans were carried out in PBS (0.05 M, pH 7.0) in the potential range from −1.0 to 1.0 V, until repetitive cyclic voltammograms (CVs) were obtained. The solution, in which nickel deposition was conducted, typically consisted of 10 ml acetate buffer (pH 4.0). The nickel was initially electrodeposited with the potential cycling method (30 cycles, 0.5 to −1.0 V) with the scan rate value of 100 mV/s on a GC electrode from a 1.0 mM nickel nitrate pH 4.0 acetate buffer solution (Fig. 1) (protocol for the NiO NPs/GC electrode) [66,67]. It has been shown previously that, the chemical dissolution of $Ni(OH)_2$ and hence the amount of passive nickel oxide formed will depend on the pH of solution. It has been suggested that in acid solution the passive film of nickel is a mixed nickel oxide film ($NiO(Ni_2O_3)$) [67]. It should be noted that the nickel oxides that both NiO and Ni_3O_4 are found to be stable species [68]. It was reported that a stable voltammograms was observed after continuous CVs. It was observed that by changing the buffer solution at pH 4.0 from acetate to phosphate had no significant effects on the passivation procedure thereby showing that the passivation is

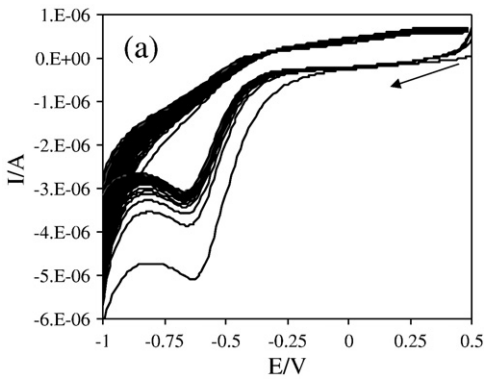

Fig. 1. Continuous CVs (30 cycles) of the NiO NPs deposition on the GC electrode in PBS (pH 4.0) containing of 1 mM Ni $(NO_3)_2.H_2O$.

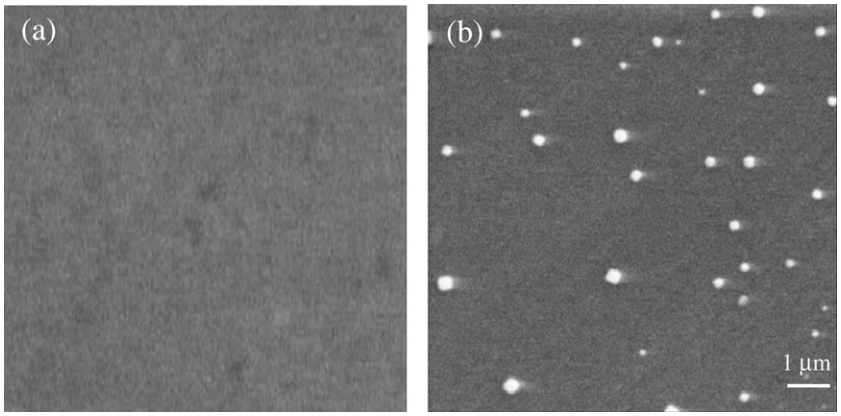

Fig. 2. (a) SEM image of the GC electrode surface before construction of nickel oxide nanoparticles, (b) SEM image of electrodeposited nickel oxide nanoparticles on the GC electrode surface.

anion independent [67]. In another protocol, the NiO NPs/GC electrode was placed into a fresh PBS including 4 mg/ml myoglobin and potentials were repetitively cycled (50 scans) from 0.7 to −0.6 V with the scan rate value of 100 mV/s. Finally, the modified electrodes were washed in deionized water and placed in PBS (pH 7.0) at a refrigerator (3–5 °C), before being employed in electrochemical measurements as the working electrode.

3. Results and discussions

3.1. Scanning Electron Microscopy (SEM) and Atomic Force Microscopy (AFM)

Fig. 2(a) shows SEM image of GC electrode surface before construction of nickel oxide nanoparticles, while Fig. 2(b) shows SEM image of the nanometer-scale nickel oxide particles, generated on the GC electrode surface in different distances from each other in various sizes.

Fig. 3(a and b) depict AFM images of the nanometer-scale nickel oxide particles. Fig. 3 (c) demonstrates the related image profile for selected direction by arrow from Fig. 3(a). This profile displayed that the nanoparticle diameters decrease on top, contrary to the bottom of nanoparticles (similar to a needle). It displays the NiO NP diameter for selected points of profile with the values of 149 and 324 nm, respectively.

3.2. Myoglobin immobilization on the electrodeposited nickel oxide nanoparticles

In the electrochemical investigations of myoglobin immobilization on the nickel oxide nanometer-scale surfaces, a

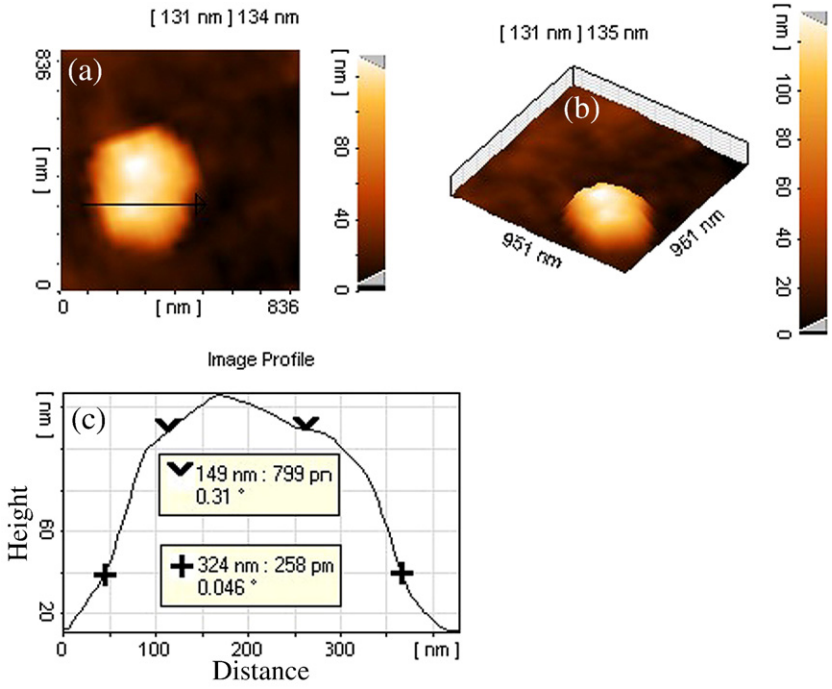

Fig. 3. (a and b) AFM images of the electrodeposited nickel oxide nanoparticles on GC electrode surface, (c) obtained image profile for selected direction by arrow from Fig. 3a.

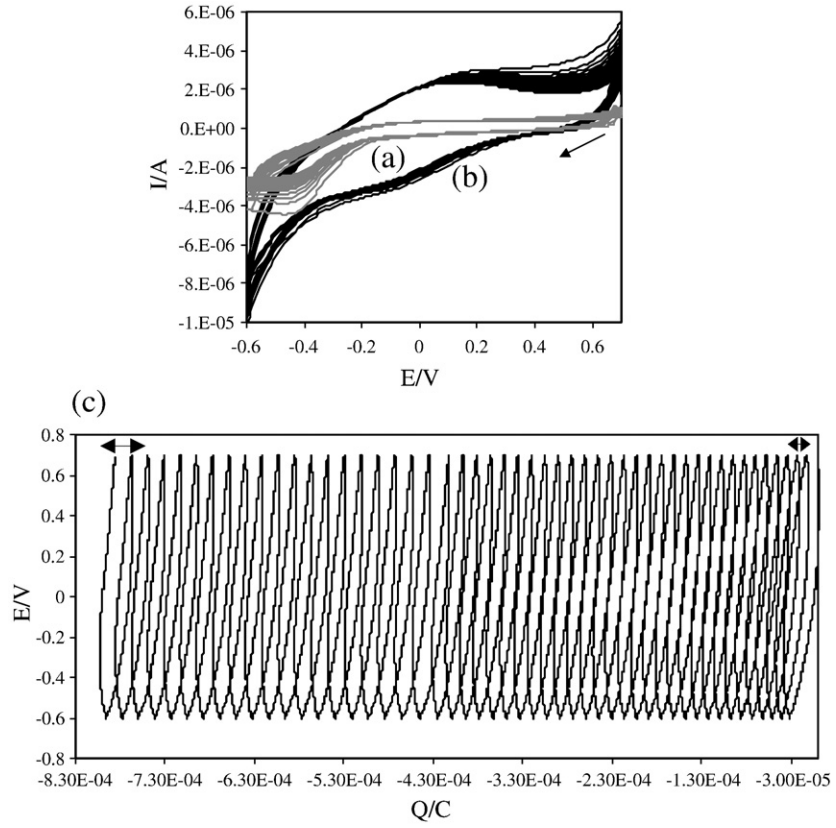

Fig. 4. NiO NPs passivation (a), NiO NPs passivation and myoglobin immobilization (b) by the potential cycling method (50 cycles) in PBS (pH 7.0), scan rate; 100 mV/s, and (c) the potentials (*E*) *vs.* the charge passed through the electrochemical cell for the simultaneous passivation of the deposited NiO NPs and the myoglobin immobilization in PBS. The data were obtained for 50 cycles (CVs presented in Fig. 3b).

potential cycling (30 cycles) was applied to the electrodeposited nickel oxide nanoparticles in the absence and presence of myoglobin, between 0.7 to −0.60 V in PBS (pH 7.0) at the scan rate of 100 mV/s. Fig. 4a demonstrates the acquired CVs in PBS (pH 7.0) for the passivity of deposited NiO NPs on the GC electrode. Fig. 4b shows the obtained CVs under the same conditions in the fresh PBS, as well as 4 mg/ml myoglobin. It was clear that the displayed faradaic response were related to the electrochemical oxidation and reduction of the immobilized myoglobin on nickel oxide nanometer-scale surfaces. The myoglobin covered the NiO NPs and stable CVs were observed. This phenomenon became more evident from the plot of *E* vs. *Q* in Fig. 4c. In this figure, the distances among the rings decreased with the consumed charges (*Q*) increase, in accordance with the increase of immobilized myoglobin and decrease of bare NiO NPs.

3.3. Voltammetric behavior of the Mb/NiO NPs/GC electrode

Integrity of immobilized myoglobin construction and its ability to exchange electrons with the NiO NPs were assessed by voltammetry. Comparative voltammograms for the GC, NiO

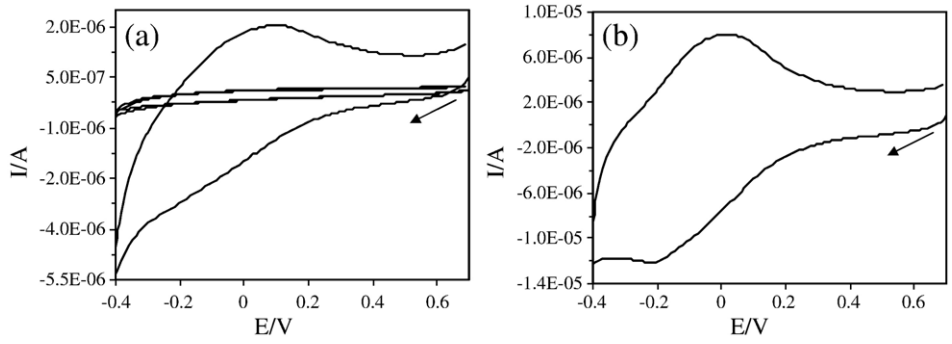

Fig. 5. (a) CVs in PBS (pH 7.0, 0.05 M) from inner to outer; GC electrode, NiO NPs/GC electrode and the Mb/NiO NPs/GC electrode, scan rate; 100 mV/s. (b) CVs of Mb/NiO NPs/GC electrode in 0.05 M PBS (pH 7.0), scan rate; 100 mV/s.

NPs/GC (GC electrode was modified with the nanometer-scale nickel oxide particles) and Mb/NiO NPs/GC electrodes in 0.05 M PBS (pH 7.0) was obtained. These voltammograms are demonstrated in Fig. 5. From this Figure, it was noticed that there were no voltammetric responses at both bare GC and GC-NiO electrodes, which indicated that the GC and NiO NPs/GC electrodes were electroinactive in the studied potential window. However, Fig. 5a depicts a well-defined pair of oxidation-reduction (redox) peaks, observed at the Mb/NiO NPs/GC electrode at scan rate value of 100 mV/s. In agreement with the collected voltammograms in Fig. 5a, it was concluded that the nanometer-scale nickel oxide particles could play a key role in the observation of myoglobin voltammetric response. These nanoparticles displayed a great effect on electron exchange assistance between myoglobin and GC electrode. Continuous cyclic voltammograms (CCVs) were applied for this electrode in PBS at 200 mV/s (150 cycles). Then, it retained in PBS (pH 7.0) at a refrigerator (3–5 °C) for a week and after this period the electrode shows better voltammetric response. The improved electrode presented its reductive peak potential at −0.228 V and its corresponding oxidative peak potential at 0.013 V (at 100 mV/s, Fig. 5b). Difference of the anodic and cathodic peak potential values was ΔE=0.241 V, whereas formal potential (an average midpoint potential of cathodic and anodic peak potential) for myoglobine redox reaction on the electrode was −0.1075 V (0.0895 vs. NHE), more positive than the potentials reported for myoglobin on nanoporous ZnO film (−0.053 V vs. NHE.0) [29], myoglobin on multi-walled carbon nanotubes (−0.007 V vs. NHE) [36], myoglobin/colloidal gold nanoparticles (−0.131 V vs. NHE) [38], Mb/Au/ITO electrode (−0.133 V vs. NHE) [39] and Mb/sol–gel (−0.101 V *vs.* NHE) [69]. In accordance with Fig. 5, magnitude of the electrochemical signal was improved for this electrode. This might have been caused by the protein concentration increase, which was in electrical communication with the NiO NP surfaces. The connectivity of protein prosthetic groups with the NiO NPs might have been affected by some rearrangements. In detail, the overall current in Fig. 5b appears to be about four times greater than that of Fig. 5a, suggesting that significant fouling of the electrode occurred, i.e. substantial structural changes at electrode/solution interface, e. g. changes to the nickel oxide structure during CCVs and over the course of a week. Additionally, the peak shape was modified.

To further investigate the myoglobin characteristics at the Mb/NiO NPs/GC electrode, effect of scan rates on the myoglobin voltammetric behavior was studied in detail and the kinetic parameters were acquired. Fig. 6(a and b) depicts the CVs for immobilized myoglobin at various scan rates. The scan rate (v) and the square root scan rate ($v^{1/2}$) vs. peak currents are plotted in Fig. 6(c and d). It can be seen that redox peak currents increased linearly with scan rate, the correlation coefficient was 0.998 (i_{pc}=−0.095 v −2.523) and 0.998 (i_{pa}=0.080 v+1.070), respectively. This phenomenon suggested that the redox process was an adsorption-controlled and the immobilized myoglobin was stable.

It was found that the peak potentials (E_{pa} and E_{pc}) and natural logarithm of scan rate (ln v) are linearly dependant in the range from 450 to 1000 mV/s, which was in agreement

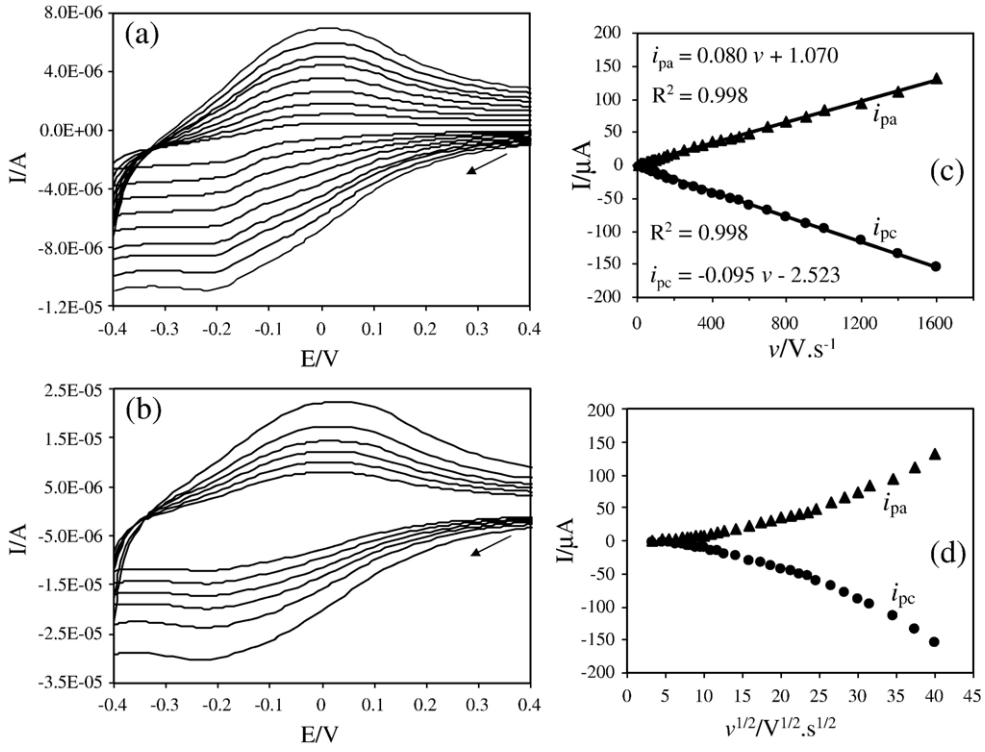

Fig. 6. CVs of Mb/NiO NPs/GC electrode in PBS (pH 7.0, 0.05 M) at various scan rates, from inner to outer; (a) 10, 20, 30, 40, 50, 60, 70, 80, 90 (b) 100, 120, 140, 160, 200 and 250 mV/s. The plot of peak currents *vs.* (c) the scan rates and (d) the square root of scan rates.

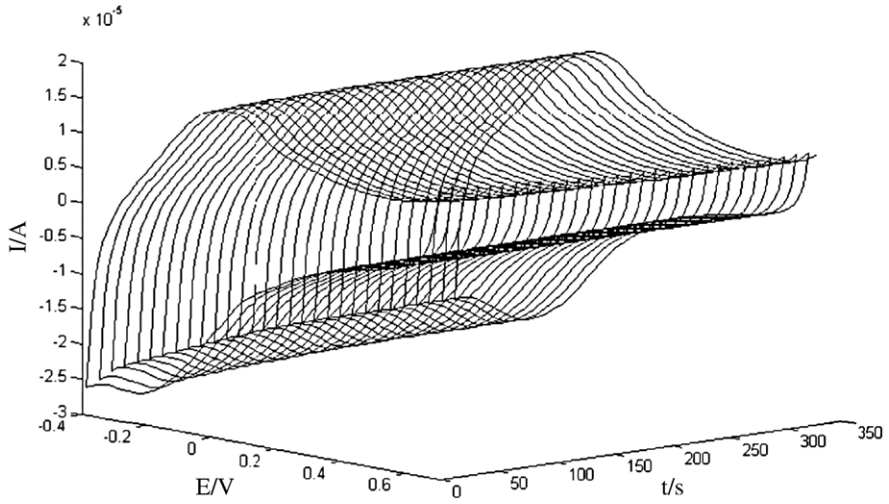

Fig. 7. Continuous CVs of Mb/NiO NPs/GC electrode in PBS, first 30 (1st–30th) voltammograms, scan rate: 200 mV/s.

with the Laviron theory [70]. The anodic peak potential (E_{pa}) changed linearly *vs.* ln v with a linear regression equation of $E_{pa}=0.0574\ \ln v+0.1074$, $R^2=0.99$. As a result, the charge transfer coefficient (α) can be estimated according to the following equation:

$$E_{pa} = E^{0'} - \frac{RT}{(1-\alpha)nF} + \frac{RT}{(1-\alpha)nF}\ln v \quad (1)$$

where α is the electron transfer coefficient, n the number of electrons, R, T and F are gas, temperature and Faraday constant, respectively. αn is calculated to be 0.55. Given $0.3<\alpha<0.7$ in general [71], it could be concluded that $n=1$ and $\alpha=0.55$. So, the redox reaction between myoglobin and NiO NP is a single electron transfer process.

In order to calculate the value of heterogeneous electron transfer rate constant (k_s), the following equation [72] was used:

$$\mathrm{Log}\, k_s = \alpha \log(1-\alpha) + (1-\alpha)\log\alpha - \log\frac{\mathrm{RT}}{nFv} - \alpha(1-\alpha)\frac{nF\Delta E_p}{2.303\,RT} \quad (2)$$

The k_s value was determined to be 0.34 s^{-1}. It was less than Mb/MWNTs modified electrode (5.4 s^{-1}) [36], Mb/nanoporous ZnO/graphite electrode (1.0 s^{-1}) [29], Mb/agarose (47±3) [73], Mb/arylhydroxylamine modified electrode (51±5) [74], Mb/hydrated poly(ester sulfonic acid) ionomer films (52±6) [75], Mb/polyacrylamide (86±19) [76] and Mb/$2C_{12}N^+Br^-$ (31±3) [77].

Stability is an important character in biodiagnostics. The stability of the Mb/NiO NPs/GC electrode was assessed by continuous cyclic voltammetry. Fig. 7 demonstrates the 1st–30th continuous cyclic voltammograms (100 cycles) of the prepared electrode. The peak height and the peak potential of the electrode were approximately unchanged during the long time continuous cyclic voltammograms from 0.70 to −0.40 V. The figure presented that there is no changes in the redox potentials.

3.4. Electrocatalytic reduction of H_2O_2 on the Mb/NiO NPs/GC electrode

The mechanism of catalytic reduction of hydrogen peroxide on the Mb/NiO NPs/GC electrode is similar to that of

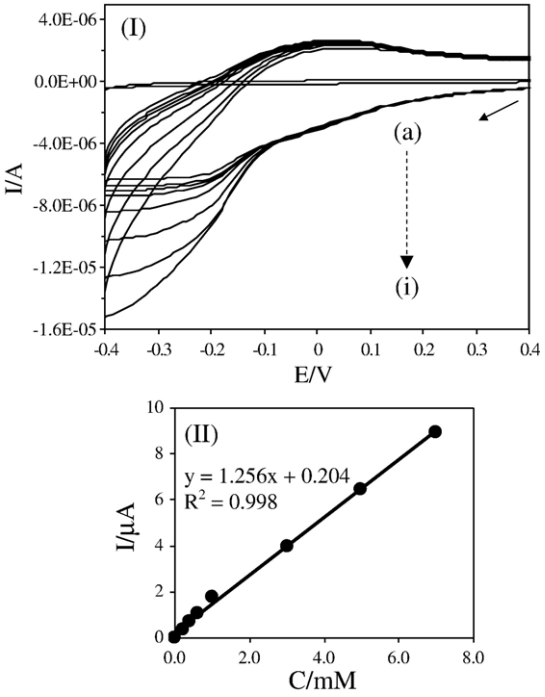

Fig. 8. (I) The obtained cyclic voltammetric response for NiO NPs/GC electrode in PBS containing 1.0 mM H_2O_2 (a), Mb/NiO NPs/GC electrode in PBS in the absence (b) and presence various concentrations of H_2O_2 at the scan rate value of 50 mV/s, 0.2 (c), 0.4 (d), 0.6 (e), 1.0 (f), 3.0 (g), 5.0 (h) and 7.0 mM (i). (II) The catalytic response versus hydrogen peroxide concentrations.

horseradish peroxidase (HRP) film system [78], as Mb and HRP are heme containing proteins that have similar electrochemical properties. The electrocatalytic process can be expressed as follow [79]:

$$\text{Mb heme Fe (III)} + H^+ + e^- \rightleftharpoons \text{Mb heme Fe (II)}$$

$$H_2O_2 + 2H^+ + 2\ \text{Mb heme Fe(II)} \longrightarrow 2\ \text{Mb heme Fe(III)} + 2H_2O$$

$$\text{Mb heme Fe(III)} + H^+ + e^- \longrightarrow \text{Mb heme Fe(II)}$$

The CVs obtained for PBS with various H_2O_2 concentrations are illustrated in Fig. 8. Fig. 8 (I, a) related to the obtained cyclic voltammetric response for NiO NPs/GC electrode in PBS containing 1.0 mM H_2O_2. As shown NiO NPs/GC electrode, no redox response of H_2O_2 can be seen in the potential range from 0.4 to −0.4 V. However, at the Mb/NiO NPs/GC electrode, reduction current of electrode was greatly increased due to catalytic reduction of hydrogen peroxide, while the oxidation peak decreased. Therefore, in order to evaluate the Mb/NiO NPs/GC electrode, cyclic voltammograms of the electrode in the presence of different concentrations of hydrogen peroxide were recorded in Fig. 8 (I, b–i). Clearly, when H_2O_2 was added to the buffer solution, the voltammetric behavior of electrode changed considerably, with an increase of reduction peak current. Decreases of the oxidative peak current together with increases of reductive peak current confirmed that myoglobin on the Mb/NiO NPs/GC electrode demonstrated a catalytic ability for H_2O_2 reduction. It is of great importance to mention that the oxidative peak did not disappear after the onset of reductive catalysis. This phenomenon could be attributed to the fact that most of adsorbed protein is probably not catalytically active. Fig. 8 (II) demonstrated that the catalytic current linearly increased with increase in the concentration of hydrogen peroxide and calibration plot is linear with correlation coefficient value of 0.998. To evaluate reproducibility of the electrode, the response of an Mb/NiO NPs/GC electrode was examined for 10 measurements in 1.0 mM H_2O_2 in PBS. The catalytic current at −0.38 V shows a relative standard deviation (%R.S.D.) with the value of 1.8%. The sensitivity and the detection limit (3σ) of the electrode towards hydrogen peroxide were found to be 1.256 μA/mM and 75 μM, respectively.

4. Conclusions

The Mb/NiO NPs were successfully assembled onto glassy carbon solid substrate. NiO nanoparticles, with their good biocompatibility and large surface area, could adsorb myoglobin on their surfaces and displayed electrochemical responses. This attractive property could open a new entrance for newly designed protein immobilized nanoparticles in biodiagnostic applications. Bioelectrochemistry of redox proteins and enzymes can provide a model for the mechanistic study of electron exchange between enzymes in the biological systems. The bioelectrochemistry of immobilized enzymes with underlying electrodes can also establish a foundation for fabricating new kinds of bioreactors and biomedical devices without using mediators. Undoubtedly, nanotechnology in combination with bioelectrochemistry can extremely influence the development rate of these scientific fields. However, a number of challenges remain to be faced, which are related to processing of electrode modifications in a more controlled method. The charge transport mechanism in nanostructured biointerfaces presents a great interest, requiring further investigation.

Acknowledgements

The authors would like to thank Mr. S.M. Hashemi for performance of the SEM studies from the Science College Electron Microscopy Laboratory, University of Tehran. Additionally, the authors wish to express their appreciation for useful comments of the referees. Moreover, the financial support provided by the University of Tehran Research Affairs is gratefully acknowledged.

References

[1] A.N. Shipway, E. Katz, I. Willner, Nanoparticle arrays on surfaces for electronic, optical, and sensor applications, Chem. Phys. Chem. 1 (2000) 18–52.
[2] T. Funatsu, Y. Harada, H. Higuchi, M. Tokunaga, K. Saito, Y. Ishii, R.D. Vale, T. Yanagida, Imaging and nano-manipulation of single biomolecules, Biophys. Chem. 68 (1997) 63–72.
[3] M.J. Bruchez, M. Moronne, P. Gin, S. Weiss, A.P. Alivisatos, Semiconductor nanocrystals as fluorescent biological labels, Science 281 (1998) 2013–2016.
[4] J.F. Hicks, F.P. Zamborini, R.W. Murray, Dynamics of electron transfers between electrodes and monolayers of nanoparticles, J. Phys. Chem., B 106 (2002) 7751–7757.
[5] L. Suber, P. Imperatori, G. Ausanio, F. Fabbri, H. Hofmeister, Synthesis, morphology, and magnetic characterization of iron oxide nanowires and nanotubes, J. Phys. Chem., B 109 (2005) 7103–7109.
[6] R. Gangopadhyay, A. De, Conducting polymer nanocomposites: A brief overview, Chem. Mater. 12 (2000) 608–622.
[7] A. Verma, V.M. Rotello, Surface recognition of biomacromolecules using nanoparticle receptors, Chem. Commun. (2005) 303–312.
[8] J. Wang, Nanomaterial-based electrochemical biosensors, Analyst 130 (2005) 421–426.
[9] I. Willner, E. Katz, Integration of layered redox proteins and conductive supports for bioelectronic applications, Angew. Chem. Int. Ed. 39 (2000) 1180–1218.
[10] A. Bayandori Moghaddam, M.R. Ganjali, R. Dinarvand, T. Razavi, A.A. Saboury, A.A. Moosavi-Movahedi, P. Norouzi, Direct electrochemistry of cytochrome *c* on electrodeposited nickel oxide nanoparticles, J. Electroanal. Chem. (2007), doi:10.1016/j.jelechem.2007.11.011.
[11] A. Bayandori Moghaddam, M.R. Ganjali, R. Dinarvand, A.A. Saboury, A.A. Moosavi-Movahedi, P. Norouzi, Fundamental studies of the cytochrome *c* immobilization by the potential cycling method on nanometer-scale nickel oxide surfaces, Biophys. Chem. 129 (2007) 259–268.
[12] Y. Xiao, F. Patolsky, E. Katz, J.F. Hainfeld, I. Willner, Plugging into enzymes, nanowiring of redox enzymes by a gold nanoparticle, Science 299 (2003) 1877–1881.
[13] D.A. Moffet, J. Foley, M.H. Hecht, Midpoint reduction potentials and heme binding stoichiometries of de novo protein from designed combinatorial libraries, Biophys. Chem. 105 (2003) 231–239.
[14] Y.-H. Bi, Z.-L. Huang, Y.-D. Zhao, Z.-L. Huang, Y.-D. Zhao, Interactions of cytochrome *c* with DNA at glassy carbon surface, Biophys. Chem. 116 (2005) 193–198.
[15] J.F. Satargardt, F.M. Hawkridge, H.L. Landrum, Reversible heterogeneous reduction and oxidation of sperm whale myoglobin at a surface modified gold minigrid electrode, Anal. Chem. 50 (1978) 930–932.

[16] D.P. Hildebrand, H.-I. Tang, Y. Luo, C.L. Hunter, M. Smith, G.D. Brayer, A.G. Mauk, Efficient coupled oxidation of heme by an active site variant of horse heart myoglobin, J. Am. Chem. Soc. 118 (1996) 12909–12915.
[17] E. Stellwagen, Haem exposure as the determinate of oxidation–reduction potential of haem proteins, Nature 275 (1978) 73–74.
[18] P. Yeh, T. Kuwana, Reversible electrode reaction of cytochrome *c*, Chem. Lett. 10 (1977) 1145–1148.
[19] M.J. Eddowes, H.A.O. Hill, Novel method for the investigation of the electrochemistry of metalloproteins: cytochrome *c*, J. Chem. Soc., Chem. Commun. 21 (1977) 771b–772b.
[20] F.A. Armstrong, G.S. Wilson, Recent developments in faradaic bioelectrochemistry, Electrochim. Acta 45 (2000) 2623–2645.
[21] L. Gorton, A. Lindgren, T. Larsson, F.D. Munteanu, T. Ruzgas, I. Gazargan, Direct electron transfer between heme-containing enzymes and electrodes as basis for third generation biosensors, Anal. Chim. Acta 400 (1999) 91–108.
[22] M. Fedurco, Redox reactions of heme-containing metalloproteins: Dynamic effects of self-assembled monolayers on thermodynamics and kinetics of cytochrome *c* electron-transfer reactions, Coord. Chem. Rev. 209 (2000) 263–331.
[23] Q. Gao, S.L. Suib, J.F. Rusling, Colloids, helices, and patterned films made from heme proteins and manganese oxide, Chem. Commun. (2002) 2254–2255.
[24] E. Topoglidis, C.J. Campbell, A.E.G. Cass, J.R. Durrant, Factors that affect protein adsorption on nanostructured titania films. A novel spectroelectrochemical application to sensing, Langmuir 17 (2001) 7899–7906.
[25] C.V. Kumar, A. Chaudhari, Proteins immobilized at the galleries of layered alpha-zirconium phosphate: structure and activity studies, J. Am. Chem. Soc. 122 (2000) 830–837.
[26] X. Xu, B.Z. Tian, J.L. Kong, S. Zhang, B.H. Liu, D.Y. Zhao, Ordered mesoporous niobium oxide film: A novel matrix for assembling functional proteins for bioelectrochemical applications, Adv. Mater. 15 (2003) 1932–1936.
[27] S. Peng, Q. Gao, Q. Wang, J. Shi, Layered structural heme protein magadiite nanocomposites with high enzyme-like peroxidase activity, Chem. Mater. 16 (2004) 2675–2684.
[28] Z. Dai, X. Xu, H. Ju, Direct electrochemistry and electrocatalysis of myoglobin immobilized on a hexagonal mesoporous silica matrix, Anal. Biochem. 332 (2004) 23–31.
[29] G. Zhao, J.-J. Xu, H.-Y. Chen, Interfacing myoglobin to graphite electrode with an electrodeposited nanoporous ZnO film, Anal. Biochem. 350 (2006) 145–150.
[30] V.V. Shumyantseva, Y.D. Ivanov, N. Bistolas, F.W. Scheller, A.I. Archakov, U. Wollenberger, Direct electron transfer of cytochrome P4502B4 at electrodes modified with nonionic detergent and colloidal clay nanoparticles, Anal. Chem. 76 (2004) 6046–6052.
[31] C.E. Immoos, J. Chou, M. Bayachou, E. Blair, J. Greaves, P.J. Farmer, Electrocatalytic reductions of nitrite, nitric oxide, and nitrous oxide by thermophilic cytochrome P450CYP119 in film-modified electrodes and an analytical comparison of its catalytic activities with myoglobin, J. Am. Chem. Soc. 126 (2004) 4934–4942.
[32] S. Boussaad, N.J. Tao, Electron transfer and adsorption of myoglobin on self-assembled surfactant films: An electrochemical tapping-mode AFM study, J. Am. Chem. Soc. 121 (1999) 4510–4515.
[33] M. Bayachou, R. Lin, W. Cho, P.J. Farmer, Electrochemical reduction of NO by myoglobin in surfactant film: characterization and reactivity of the nitroxyl (NO-) adduct, J. Am. Chem. Soc. 120 (1998) 9888–9893.
[34] V. Panchagnula, C.V. Kumar, J.F. Rusling, Ultrathin layered myoglobin-polyion films functional and stable at acidic pH values, J. Am. Chem. Soc. 124 (2002) 12515–12521.
[35] H. Liu, N.J. Hu, Selective oxidation of methanol and ethanol on supported ruthenium oxide clusters at low temperatures, J. Phys. Chem. B 109 (2005) 10464–10473.
[36] G.C. Zhao, L. Zhang, Q.W. Wei, Z.S. Yang, Myoglobin on multi-walled carbon nanotubes modified electrode: direct electrochemistry and electrocatalysis, Electrochem. Commun. 5 (2003) 825–829.
[37] L. Zhao, H. Lin, N. Hu, Assembly of layer-by-layer films of heme proteins and single-walled carbon nanotubes, Anal. Bioanal. Chem. 384 (2006) 414–422.
[38] W. Yang, Y. Li, Y. Bai, C. Sun, Hydrogen peroxide biosensor based on myoglobin/colloidal gold nanoparticles immobilized on glassy carbon electrode by a Nafion film, Sens. Actuators, B 115 (2006) 42–48.
[39] J. Zhang, M. Oyama, Gold-nanoparticle-attached ITO as a biocompatible matrix for myoglobin immobilization: direct electrochemistry and catalysis to hydrogen peroxide, J. Electroanal. Chem. 577 (2005) 273–279.
[40] J. Zhang, M. Oyama, Electroanalysis of myoglobin and hemoglobin with a boron-doped diamond electrode, Microchem. J. 78 (2004) 217–222.
[41] G. Wang, H. Lu, N. Hu, Electrochemically and catalytically active layer-by-layer films of myoglobin with zirconia formed by vapor-surface sol–gel deposition, J. Electroanal. Chem. 599 (2007) 91–99.
[42] E.V. Ivanova, E. Magner, Direct electron transfer of haemoglobin and myoglobin in methanol and ethanol at didodecyldimethylammonium bromide modified pyrolytic graphite electrodes, Electrochem. Commun. 7 (2005) 323–327.
[43] A. Bayandori Moghaddam, M.R. Ganjali, R. Dinarvand, P. Norouzi, A.A. Saboury, A.A. Moosavi-Movahedi, Electrochemical behavior of caffeic acid at single-walled carbon nanotube:graphite-based electrode, Biophys. Chem. 128 (2007) 30–37.
[44] E. Katz, I. Willner, Integrated nanoparticle-biomolecule hybrid systems: synthesis, properties, and applications, Angew. Chem. Int. Ed. 43 (2004) 6042–6108.
[45] B.E. Conway, M.A. Sattar, D. Gilroy, Electrochemistry of the nickel-oxide electrode — V. Self-passivation effects in oxygen-evolution kinetics, Electrochim. Acta 14 (1969) 677–694.
[46] B.E. Conway, M.A. Sattar, Electrochemistry of the nickel oxide electrode : Part VIII. Stoichiometry of thin film oxide layers, J. Electroanal. Chem. 19 (1968) 351–364.
[47] M. Fleischmann, K. Korinek, D. Pletcher, The oxidation of organic compounds at a nickel anode in alkaline solution, J. Electroanal. Chem. 31 (1971) 39–49.
[48] J.V. Dobson, B.R. Chapman, The electrode kinetic behaviour of nickel in aqueous stearic acid salt media up to 210 °C, Electrochim. Acta 32 (1987) 415–418.
[49] G. Cordeiro, O.R. Matos, O.E. Barcia, L. Beaunier, C. Deslouis, B. Tribollet, Anodic dissolution of nickel in concentrated sulfuric acidic solutions, J. Appl. Electrochem. 26 (1996) 1083–1092.
[50] M.R. Barbosa, S.G. Real, J.R. Vilche, A.J. Arvia, Comparative potentiodynamic study of nickel in still and stirred sulfuric acid-potassium sulfate solutions in the 0.4–5.7 pH range, J. Electrochem. Soc. 135 (1988) 1077–1084.
[51] M.R. Barbosa, J.A. Bastos, J.J. Gracia-Jareno, F. Vicente, Chloride role in the surface of nickel electrode, Electrochim. Acta 44 (1998) 957–965.
[52] R.S. Schrebler Guzman, J.R. Vilche, A.J. Arvia, Electrochemical and chemical reactions involving non-equilibrium species at the nickel hydroxide electrode, J. Appl. Electrochem. 9 (1979) 321–327.
[53] D. Giovanelli, N.S. Lawrence, L. Jiang, T.G.J. Jones, R.G. Compton, Electrochemical determination of sulphide at nickel electrodes in alkaline media: A new electrochemical sensor, Sens. Actuators, B 88 (2003) 320–328.
[54] D. Giovanelli, N.S. Lawrence, L. Jiang, T.G.J. Jones, R.G. Compton, Amperometric determination of sulfide at a pre-oxidised nickel electrode in acidic media, Analyst 128 (2003) 173–177.
[55] R.D. Tilley, D.A. Jefferson, The synthesis of nickel sulfide nanoparticles on graphitized carbon supports, J. Phys. Chem., B 106 (2002) 10895–10901.
[56] J.L. Wong, M. Tian, W.R. Jin, Y.N. He, Speciation of sulfidic nickel by carbon paste electrode voltammetry. Determination of Ni_3S_2 in solid mixtures, Electroanalysis 12 (2001) 1355–1359.
[57] D. Giovanelli, N.S. Lawrence, S.J. Wilkins, L. Jiang, T.G.J. Jones, R.G. Compton, Anodic stripping voltammetry of sulphide at a nickel film: towards the development of a reagentless sensor, Talanta 61 (2003) 211–220.
[58] A. Salimi, E. Sharifi, A. Noorbakhsh, S. Soltanian, Direct voltammetry and electrocatalytic properties of hemoglobin immobilized on a glassy carbon electrode modified with nickel oxide nanoparticles, Electrochem. Commun. 8 (2006) 1499–1508.
[59] A. Salimi, E. Sharifi, A. Noorbakhsh, S. Soltanian, Direct electrochemistry and electrocatalytic activity of catalase immobilized onto electrodeposited nano-scale islands of nickel oxide, Biophys. Chem. 125 (2007) 540–548.

[60] A. Salimi, E. Sharifi, A. Noorbakhsh, S. Soltanian, Immobilization of glucose oxidase on electrodeposited nickel oxide nanoparticles: direct electron transfer and electrocatalytic activity, Biosens. Bioelectron. 22 (2007) 3146–3153.
[61] C. Mu, Q. Zhao, D. Xu, Q. Zhuang, Y. Shao, Silicon nanotube array/gold electrode for direct electrochemistry of cytochrome *c*, J. Phys. Chem., B 111 (2007) 1491–1495.
[62] A. Bayandori Moghaddam, F. Kobarfard, A.R. Fakhari, D. Nematollahi, S.S. Hosseiny Davarani, Mechanistic study of electrochemical oxidation of *o*-dihydroxybenzenes in the presence of 4-hydroxy-1-methyl-2(1H)-quinolone: application to the electrochemical synthesis, Electrochim. Acta 51 (2005) 739–744.
[63] A. Bayandori Moghaddam, F. Kobarfard, S.S. Hosseiny Davarani, D. Nematollahi, M. Shamsipur, A.R. Fakhari, Electrochemical study of 3,4-dihydroxybenzoic acid in the presence of 4-hydroxy-1-methyl-2 (1H)-quinolone: application to electrochemical synthesis of new benzofuran derivative, J. Electroanal. Chem. 586 (2006) 161–166.
[64] A. Bayandori Moghaddam, M.R. Ganjali, P. Norouzi, M. Latifi, A green method for the electroorganic synthesis of new 1,3-indandione derivatives, Chem. Pharm. Bull. 54 (2006) 1391–1396.
[65] A. Bayandori Moghaddam, M.R. Ganjali, P. Norouzi, M. Niasari, A green method on the electro-organic synthesis of new caffeic acid derivatives: Electrochemical properties and LC–ESI–MS analysis of products, J. Electroanal. Chem. 601 (2007) 205–210.
[66] D. Giovanelli, N.S. Lawrence, S.J. Wilkins, L. Jiang, T.G.J. Jones, R.G. Compton, Anodic stripping voltammetry of sulphide at a nickel film: Towards the development of a reagentless sensor, Talanta 61 (2003) 211–220.
[67] D. Giovanelli, N.S. Lawrence, L. Jiang, T.G.J. Jones, R.G. Compton, Amperometric determination of sulfide at a pre-oxidised nickel electrode in acidic media, Analyst 128 (2003) 173–177.
[68] R.L. Cowan, R.W. Staehle, Thermodynamic and Electrode Kinetic, J. Electrochem. Soc. 118 (1971) 557–568.
[69] Q. Wang, G. Lu, B. Yang, Myoglobin/sol–gel film modified electrode: Direct electrochemistry and electrochemical catalysis, Langmuir 20 (2004) 1342–1347.
[70] E. Laviron, Adsorption, autoinhibition and autocatalysis in polarography and in linear potential sweep voltammetry, J. Electroanal. Chem. 52 (1974) 355–393.
[71] H.Y. Ma, N.F. Hu, J.F. Rusling, Electroactive myoglobin films grown layer-by-Layer with poly(styrenesulfonate) on pyrolytic graphite electrodes, Lungmuir 16 (2000) 4969–4975.
[72] E. Laviron, General expression of the linear potential sweep voltammograms in the case of diffusion less electrochemical systems, J. Electroanal. Chem. 101 (1979) 19–28.
[73] H.H. Liu, Z.Q. Tian, Z.X. Lu, Z.L. Zhang, M. Zhang, D.W. Pang, Direct electrochemistry and electrocatalysis of heme-proteins entrapped in agarose hydrogel films, Biosens. Bioelectron. 20 (2004) 294–304.
[74] S. Ashok Kumar, S.-M. Chen, Direct electrochemistry and electrocatalysis of myoglobin on redox-active self-assembling monolayers derived from nitroaniline modified electrode, Biosens. Bioelectron. 22 (2007) 3042–3050.
[75] N. Hu, J.F. Rusling, Electrochemistry and catalysis with myoglobin in hydrated poly(ester sulfonic acid) ionomer films, Langmuir 13 (1997) 4119–4125.
[76] L. Shen, R. Huang, N. Hu, Myoglobin in polyacrylamide hydrogel films: direct electrochemistry and electrochemical catalysis, Talanta 56 (2002) 1131–1139.
[77] A-E.F. Nassar, Z. Zhang, N. Hu, J.F. Rusling, T.F. Kumosinski, Proton-coupled electron transfer from electrodes to myoglobin in ordered biomembrane-like films, J. Phys. Chem., B 101 (1997) 2224–2231.
[78] R. Huang, N.-F. Hu, Direct electrochemistry and electrocatalysis with horseradish peroxidase in eastman AQ films, Bioelectrochemistry 54 (2001) 75–81.
[79] S.-J. Dong, Q.-H. Chu, Study on electrode process of myoglobin at a polymerized toluidine blue film electrode, Chin. J. Chem. 11 (1993) 12–20.